Fault Adaptive Control of Overactuated Systems Using Prognostic Estimation

Brian M. Bole [1], **Douglas W. Brown** [1], **Hai-Long Pei** [2], **Kai Goebel** [3], **Liang Tang** [4], **and George Vachtsevanos** [1]

[1] *Department of Electrical and Computer Engineering, Georgia Institute of Technology, Atlanta, GA, 30332, USA.*
bbole3@gatech.edu
dbrown31@gatech.edu
gjv@ece.gatech.edu
[2] *Department of Automation at South China University of Technology, Guagzhou 510640 P.R. China*
auhlpei@scut.edu.cn
[3] *NASA Ames Research Center, Moffett Field, CA 94035, USA.*
kai.goebel@nasa.gov
[4] *Impact Technologies, LLC, Rochester, NY 14623, USA.*
Liang.Tang@impact-tek.com

ABSTRACT

Most fault adaptive control research addresses the preservation of system stability or functionality in the presence of a specific failure (fault). This paper examines the fault adaptive control problem for a generic class of incipient failure modes, which do not initially affect system stability, but will eventually cause a catastrophic failure to occur. This risk of catastrophic failure due a component fault mode is some monotonically increasing function of the load on the component. Assuming that a probabilistic prognostic model is available to evaluate the risk of incipient fault modes growing into catastrophic failure conditions, then fundamentally the fault adaptive control problem is to adjust component loads to minimize risk of failure, while not overly degrading nominal performance. A methodology is proposed for posing this problem as a finite horizon constrained optimization, where constraints correspond to maximum risk of failure and maximum deviation from nominal performance. Development of the methodology to handle a general class of overactuated systems is given. Also, the fault adaptive control methodology is demonstrated on an application example of practical significance, an electro-mechanical actuator (EMA) consisting of three DC motors geared to the same output shaft. Similar actuator systems are commonly used in aerospace, transportation, and industrial processes to actuate critical loads, such as aircraft control surfaces. The fault mode simulated in the system is a temperature dependent motor winding insulation degradation.

1. INTRODUCTION

This research examines the fault adaptive control problem for systems that may have multiple components and multiple embedded controllers. An architecture is developed, which generates diagnostic and prognostic estimates on-line and operates on the system's nominal control inputs to ensure that specifications on maximum allowable risk of failure and maximum deviation from nominal performance are satisfied over a prognostic horizon.

Enforcing the performance constraint in terms of maximum allowable adjustments to the system's nominal control requires knowledge of the physical relationship between the output of the system and the inputs to each of the constituent component controllers. This research assumes an accurate model for the multi-component system is known, but the approach could be extended to handle models adapted online to capture changing system dynamics during incipient failure conditions as in (Zhank & Jiang, 2002).

Similarly, the prognostic constraint is enforced in terms of a maximum allowable loading profile on each of the system's components, which requires inverting the relationship between component loading and component degradation. However, unlike the system model, the prognostic model is assumed to have significant uncertainty. This uncertainty is handled directly by using probability density functions (pdfs) to represent fault estimates, the form of which will depend on the particular fault mode being studied, uncertainty in the prognostic model, and measurement uncertainty. The prognostic model can be generated from data or heuristic approximation. The only requirement is that the model translates an expected load on a component over the prognostic horizon into a pdf estimate of component degra-

dation at the end of the prognostic horizon. For simple systems, empirical degradation models may be used as a basis for producing prognostic pdfs. For example (Orchard, 2007) uses Paris' Law to update pdfs for crack growth. Other examples of online adaptation of prognostic models are found in (Arulampalam, Maskell, Gordon, & Clapp, 2002; Li, Kurfess, & LIANG, 2000; Brown, Georgoulas, Bae, et al., 2009).

Assuming that satisfactory system and prognostic models exist and control profiles can be found to satisfy the performance and prognostic constraints, then the fault adaptive control architecture will attempt to minimize a given cost function that captures the relative importance of minimizing risk and maximizing system performance. This paper examines how the fault adaptive control problem may be posed as a bounded optimization for a general class of overactuated systems. First the approach is described for a general system, then the implementation of the control architecture is presented for a specific application example.

The application example is an electro-mechanical actuator (EMA) consisting of three DC motors geared to the same output shaft. In this system the load is shared by three mechanically coupled motors, constituting an active redundant arrangement. The active redundant motor arrangement in the EMA will simplify the control allocation problem and allow a more easily understandable development of performance and prognostic metrics. However, the developed metrics are intended to be extended to other overactuated systems, without active redundancy. Also, demonstrating fault adaptive control development on an EMA is valuable in it's own right, because similar systems are commonly used in aerospace and industrial processes, where system failure would be extremely costly and possibly dangerous. Diagnostic and prognostic studies for similar systems are discussed in (Brown, Georgoulas, Bole, et al., 2009; Brown, Edwards, Georgoulas, Zhang, & Vachtsevanos, 2008; Zhang et al., 2008).

2. A HIERARCHICAL CONTROL ARCHITECTURE

The proposed fault adaptive control architecture is intended to supplement a nominal control system that performs adequately under nominal operating conditions. A control hierarchy is used to distribute the control effort based on high level mission objectives and low level diagnostics and prognostics. A similar hierarchical control methodology is presented in (Brown, Georgoulas, Bole, et al., 2009). The hierarchical approach breaks down the generic fault adaptive control task into sub-problems with different scopes, enabling a more formalized treatment of algorithm specifications.

The control hierarchy shown in Figure 1, is separated into three levels: the high level acts on a collection of subsystems, the middle level acts on a collection of components within a subsystem, and the low level manages individual components. This paper will analyze control of a collection of components, or the middle level of the control hierarchy. At the subsystem level, the fault adaptive control problem is identical for a wide range of applications: The subsystem is commanded to follow some mission profile within performance and prognostic constraints. If the constraints turn out to be unsatisfiable,
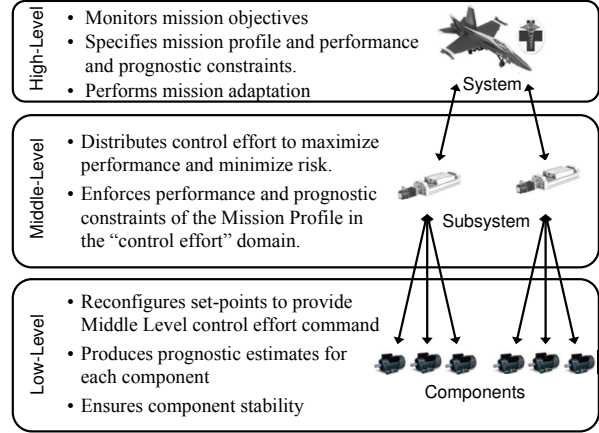

Figure 1: Description of high, middle, and low levels of the hierarchical fault adaptive control architecture

then the high level must analyze the overall objectives of the system and perform mission adaptation, as described in (Drozeski, 2005). If the constraints are satisfiable then the middle level will attempt to find an optimal control effort assignment for the subsystem's components. These component control effort commands are translated into set point modifications by the low level of the fault adaptive control system; model predictive control is commonly used to this end, as in (Monaco, Ward, & Bateman, 2004).

Figures 2 and 3 show block diagrams for a subsystem under nominal control and for a subsystem with an adaptive hierarchical control, respectively; the symbols used in these figures are defined in the Nomenclature section at the end of the paper. The figure depicting the nominal subsystem shows the basic structure assumed for the subsystem under nominal control. Here, each component is assumed to have an embedded controller that updates a component control vector, $\mathbf{u}_i$, based on the difference between the commanded state vector, θ_c, and a feedback vector, θ_o. The mapping between the loads on each of the system's components, $\mathbf{y}_i$, and the total output force exerted by the system on an external load, $\mathbf{y}$, is represented by $h(\cdot)$. This physical mapping is assumed to be known, however it is allowed to be dynamic and nonlinear. If the system is overactuated, then this mapping
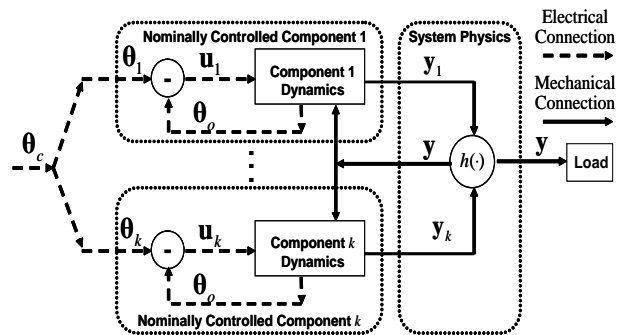

Figure 2: Shows the passing of control signals for a nominally controlled subsystem.
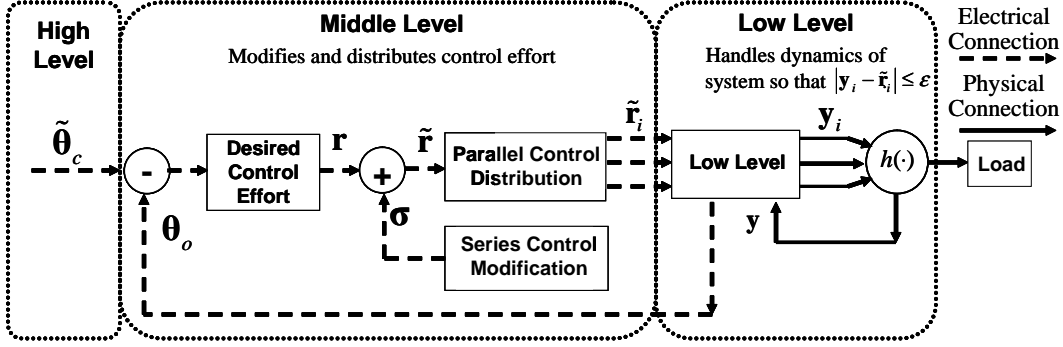
Figure 3: Shows the passing of control signals between high, middle, and low levels for the fault adaptive controller

will not be one-to-one, so there may be one or more degrees of freedom assigning load profiles to each of the system's components for a given desired system output. As shown in Figure 3, the hierarchical controller solves an optimal control effort distribution problem, where the optimal subsystem control effort output, $\tilde{r}$, is selected first, and then the optimal component control efforts, $\tilde{r}_i$, are selected.

3. CONTROL DISTRIBUTION AS A BOUNDED OPTIMIZATION PROBLEM

For some systems the middle and low level control routines can be made such that the middle level is essentially able to directly control component loads. This simplifying assumption is written as, $|y_i - \tilde{r}_i| \leq \epsilon$, where ϵ is sufficiently small. If this assumption is valid, then the middle level control effort distribution problem can be solved using standard optimal control allocation methods, as in (Harkegard & Glad, 2005; Oppenheimer, Doman, & Bolender, 2006; .M.Zhang & J.Jiang, 2002).

Figure 4 shows a reduced order subsystem model, where the low level dynamics have been replaced with an error term, δ_i. Specifications on δ_i and ϵ to ensure system stability and model fidelity are maintained should be developed on an application by application basis. Without loss of generality, δ and ϵ are set to zero to simplify the notation in the derivation of the middle level optimization problem, however adding nonzero parameters to the equations is straightforward.

The optimization problem at the middle level is written in terms of a cost function that penalizes performance loss and component degradation. An example cost function profiles is:

$$J(\mathbf{y}, \mathbf{y}_i) = J_p(\mathbf{y} - \tilde{\mathbf{r}}) + \lambda \cdot J_d \left(p \left(\mathbf{d}_i \left(\tau \right) | \mathbf{y}_i \left(t \right) \right) \right) \quad (1)$$

where $J_p(\mathbf{y} - \tilde{\mathbf{r}})$ penalizes the expected performance loss, $J_d \left(p \left(\mathbf{d}_i \left(\tau \right) | \mathbf{y}_i \left(t \right) \right) \right)$ penalizes the expected degradation of components, and λ is a weight that captures the relative importance of performance and reliability.

The performance inequality constraints are enforced in terms of a maximum allowable deviation from the state vector commanded by the mission profile,

$$|\{\theta_c(t)\}_i - \{\theta_o(t)\}_i| \leq \Delta_i(t) \quad (2)$$

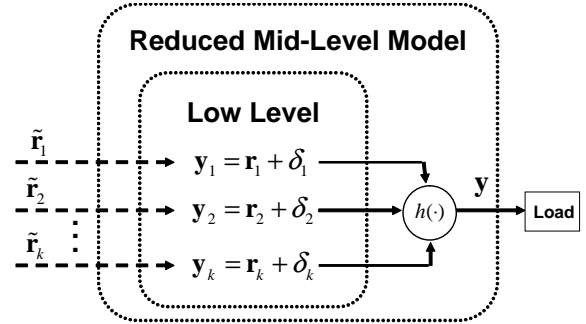where the constraint is enforced on each dimension of

Figure 4: A reduced order system model obtained using the assumption: $\mathbf{y}_i = \mathbf{r}_i + \delta_i$, and $|\mathbf{y}_i - \tilde{\mathbf{r}}_i| \leq \epsilon$

the state vector independently. For example, if the mission profile is commanding roll, pitch, and yaw of an aircraft as a function of time, then each of these dimensions will have a maximum allowable error tolerance, Δ_i.

This constraint is transformed into the control effort domain to be used as a constraint for the middle level control distribution routine,

$$|\{\mathbf{y}(t)\}_i - \{\mathbf{r}(t)\}_i| \leq \tilde{\Delta}_i(t) \quad (3)$$

The prognostic constraint, given below, places an upper bound on the probability that a component will become damaged by more than a specified amount,

$$p \left(d_i \left(\tau \right) > \phi_i \left(\tau \right) | y_i \left(t \right) \right) \leq \alpha \quad (4)$$

where $d_i \left(\tau \right)$ is the degradation of component i at time τ, $\phi_i \left(\tau \right)$ is the maximum allowable fault dimension at time τ, and α is the upper bound on the probability that the fault dimension of component i is larger than its maximum allowable value at time τ,

The prognostic constrain is also able to handle specifications in terms of a minimum allowable time to failure (TTF) or remaining useful life (RUL). Figure 5 (a) shows how the RUL constraint could be verified directly by extending the prognostic pdf all the way to a failure condition, however the uncertainty in predicting over long time horizons may be very large. Another method for incorporating the RUL constrains uses a specified maximum allowable fault growth curve and a finite horizon prediction, shown in Figure 5 (b).
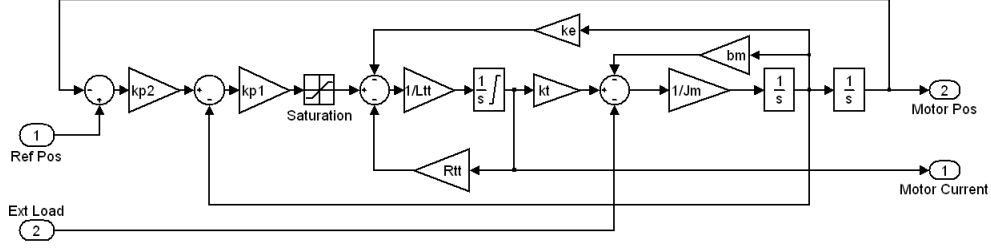
Figure 5: Evaluation of component RUL constraint in terms of long term predictions (a) and a finite horizon predictions (b)

The performance and prognostic constraints, and the cost function described in this section are used to set up the middle level control distribution as a bounded optimization problem. In the following sections, an application example is used to demonstrate the process of setting up and solving the bounded optimization problem for a real system.

4. EMA APPLICATION EXAMPLE

An electro-mechanical actuator (EMA) consisting of three DC motors geared to the same output shaft, is used to demonstrate the implementation of the control distribution architecture on an overactuated system.

4.1 EMA Model

A Simulink model for the nominal EMA system, which includes embedded position controllers on each of the three motors is given in Figure 6. Simulink models for the motors and the coupling between motors and load are shown in Figures 7 and 8, respectively. The corresponding state equations for the nominal system are given in Eq. (5) and Eq. (6). The coefficients in the EMA model are defined in Table 1. External torque on the EMA is included in the model with the variable: Q.

$$\dot{x} = A(x) + B(x)u, \; y = Cx$$

$$u = \begin{bmatrix} \theta_{r1} & \theta_{r2} & \theta_{r3} \end{bmatrix}^T \quad (5)$$

$$x = \begin{bmatrix} i_1 & i_2 & i_3 & \theta_M & \omega_M & \theta_L & \omega_L \end{bmatrix}^T$$

Figure 6: Active redundant EMA model

Figure 8: Load model for EMA

$$A = \begin{bmatrix} \dfrac{-k_{p1}k_{p2}\theta_M - \omega(k_{p1}-k_e) - R_t i_1}{L_{tt}} \\ \dfrac{-k_{p1}k_{p2}\theta_M - \omega(k_{p1}-k_e) - R_t i_1}{L_{tt}} \\ \dfrac{-k_{p1}k_{p2}\theta_M - \omega(k_{p1}-k_e) - R_t i_1}{L_t} \\ \omega_M \\ \dfrac{k_t(i_1+i_2+i_3) - 3b_M\omega_M}{3J_M} - \dfrac{k_S(\theta_M - N_M N_L \theta_L)}{J_M N_M^2} \\ \omega_L \\ \dfrac{3N_L k_S \theta_M}{N_M J_L} - \dfrac{\left(k_L + 3N_L^2 k_S\right)\theta_L - b_L\omega_L - Q}{J_L} \end{bmatrix}$$

$$B = \begin{bmatrix} \dfrac{k_{P1}k_{P2}}{L_t} & 0 & 0 \\ 0 & \dfrac{k_{P1}k_{P2}}{L_t} & 0 \\ 0 & 0 & \dfrac{k_{P1}k_{P2}}{L_t} \\ 0 & 0 & 0 \\ 0 & 0 & 0 \\ 0 & 0 & 0 \\ 0 & 0 & 0 \end{bmatrix}$$

$$C = \begin{bmatrix} 1 & 0 & 0 & 0 & 0 & 0 & 0 \\ 0 & 1 & 0 & 0 & 0 & 0 & 0 \\ 0 & 0 & 1 & 0 & 0 & 0 & 0 \end{bmatrix}$$

(6)

4

Figure 7: Motor model for EMA

Table 1: List of symbols used in EMA models

Sym	Description	Units	Value
b_L	Load damping	in·lbf/rad/s	2.5×10^{-1}
b_M	Motor damping	in·lbf/rad/s	1×10^{-4}
i_M	Motor current	A	-
k_S	Coupling stiffness	in·lbf/rad/s	1×10^{5}
k_e	Back-emf coef.	V/rad/s	1.1×10^{-1}
k_L	Load stiffness	in·lbf/rad/s	2×10^{-3}
k_{p1}	Motor speed gain	V/rad/s	1
k_{p2}	Motor position gain	s^{-1}	1
k_t	Motor torque coef.	in·lbf/A	1.01
J_L	Load inertia	in·lbf·s^2	2×10^{-3}
J_M	Motor inertia	in·lbf·s^2	2×10^{-3}
L_t	Turn-to-turn induct.	H	2×10^{-4}
N_L	Load coupling	-	1
N_M	Motor coupling	-	8
ρ	gearing ratio		8
R_t	Turn-to-turn resist	Ω	1.6×10^{-1}
θ_L	Load position	rad	-
θ_M	Motor position	rad	-
ω_L	Load speed	rad/s	-
ω_M	Motor speed	rad/s	-

4.2 Interfacing Between EMA and Middle Level Control Effort Distribution Routine

The middle level will take in a load speed command

$$|\omega_c - \omega_o| \leq \Delta(t) \tag{7}$$

This speed command is transformed into a net control effort output command and associated constraint, where torque is used as the control effort variable:

$$|T_c - T_o| \leq \tilde{\Delta}(t) \tag{8}$$

A low level controller is required to translate the middle level control effort commands into the control inputs of the embedded controllers; low level control was derived for the EMA model using dynamic inversion in (Bole, Brown, & Vachtsevanos, 2010). Assuming a low level control exists such that there is negligible error between middle level torque commands and actual motor torques, then Eq. (5) and Eq. (6) can be rewritten in the reduced form shown in Eq. (9) and Eq. (10).

$$\dot{x} = A(x) + B(x)u, \ y = Cx$$

$$x = \begin{bmatrix} \theta_L & \omega_L \end{bmatrix}^T, \ u = \begin{bmatrix} T_1 & T_2 & T_3 \end{bmatrix}^T \tag{9}$$

$$y = T_o$$

$$A(x) = \begin{bmatrix} \omega_L \\ \frac{k_L \theta_L - b_l - b_M \rho^2 \omega_L - Q}{J_L + 3\rho J_M} \end{bmatrix}$$

$$B(x) = \frac{\rho}{J_L + 3\rho J_M} \begin{bmatrix} 0 & 0 & 0 \\ 1 & 1 & 1 \end{bmatrix} \tag{10}$$

$$C = \begin{bmatrix} \rho & \rho & \rho \end{bmatrix}$$

The resulting reduced order middle level model uses motor torque directly as an input.

4.3 Prognostic Modeling

Winding insulation breakdown is a primary failure mechanism for the EMA's motors. The rate of motor winding insulation breakdown is a function of winding temperature. The standard heuristic model for this function is the ten-degree rule, introduced in 1930 by Montsinger (Montsinger, 1930). This rule states that the thermal life of insulation is halved for each increase of $10°\mathrm{K}$ in the exposure temperature. The insulation life versus temperature curve used in our simulations is given in Eq. (11),

$$L_N(t) = \alpha e^{-\beta T_W(t)} \tag{11}$$

where L_N is the expected remaining useful life (RUL) for new insulation in seconds, $T_W(t) \ (°C)$ is the winding temperature at time t, $\alpha = 10^{12}$ (s), and $\beta = 0.0693 \ (1/°C)$.

The RUL estimate for a motor winding, $L(t)$, is calculated using Eq. (12),

$$L(t) = L_N(t) \cdot \left(1 - \frac{d(t)}{100}\right) \tag{12}$$

where $d(t)$ is the percentage of insulation lifetime used prior to time t,

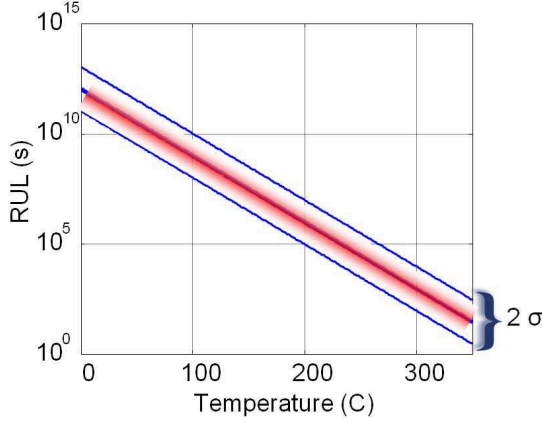$$d(t) = \int_0^t \frac{d\tau}{L(\tau)} \tag{13}$$

5

Figure 9: Addition of uncertainty pdf to the insulation breakdown model

A probability distribution is added to the α coefficient in Eq. (11) to capture uncertainty in the prognostic model. Figure 9 shows the resulting probabilistic insulation life versus temperature model, where the pdf's mean corresponds to $\alpha = 10^{12}$, one standard deviation above the mean is $\alpha = 10^{13}$, and one standard deviation below the mean is $\alpha = 10^{11}$.

4.4 Thermal Model

The winding's temperature is related to the power loss in the copper windings. A first order thermo-electrical model is used to track the winding-to-ambient temperature as a function of copper losses, as shown in Figure 10 (Nestler & Sattler, 1993). The differential equation for the thermal model is

$$\dot{T}_{wa} = -\frac{T_{wa}(t)}{R_{wa}C_{wa}} + \frac{P_{loss}(t)}{C_{wa}} \qquad (14)$$

where T_{wa} is winding-to-ambient temperature, P_{loss} is power loss in the copper windings, C_{wa} is thermal capacitance, and R_{wa} is thermal resistance.
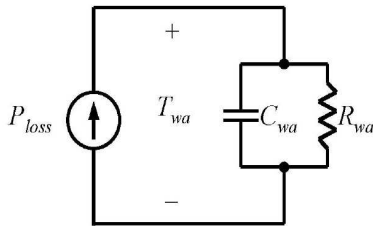
Figure 10: Thermal model for motor windings

5. SOLVING FOR THE OPTIMAL CONTROL

This section examines the optimization problem for control effort distribution among the EMA's three motors. A cost function, defined in Eq. (15), penalizes the expected deviation from the commanded output torque over the prognostic horizon and expected component damage at the end of the prognostic horizon.

$$J = \int_t^{t+\tau} |T_c - \rho\,(T_1 + T_2 + T_3)|\,dz$$

$$+ \lambda \sum_{i=1}^{3} p\,(d_i\,(t+\tau) > \psi_i\,(t+\tau)\,|T_i\,(t)) \quad (15)$$

Example performance and prognostic constraints are defined in Eq. (16) and Eq. (17), respectively.

$$0.8 \cdot T_c \leq T_o \leq T_c/0.8 \qquad (16)$$

$$p\,(d_i\,(t+\tau) > \phi_i\,(t+\tau)\,|T_i\,(t)) \leq 0.02 \qquad (17)$$

5.1 Verifying Constraint Feasibility

If the maximum allowable torque on the EMA satisfying the prognostic constraint is sufficient to satisfy the performance constraint, then the constraints are feasible. The maximum allowable torque from each motor is defined as,

$$\tilde{T}_i = \sup\,(T_i)\,,\text{s.t. } p\,(d_i\,(t+\tau) > \phi_i)\ \leq\ 0.02 \quad (18)$$

Equation (19) is used to verify that the performance constraint is feasible,

$$\left|\tilde{T}\right| \geq .8\,|T_c|\,,\ \text{where } \tilde{T} = \rho\left(\tilde{T}_1 + \tilde{T}_2 + \tilde{T}_3\right) \qquad (19)$$

Arbitrarily precise approximations for the $\tilde{T}_i$ are easily found via a wide variety of numerical techniques, given that $p\,(d_i\,(t+\tau) > \phi_i\,(t+\tau)\,|T_i\,(t))$ is monotonically increasing function of $\tilde{T}_i$.

If the constraints are infeasible, then the motor torques are chosen to satisfy the prognostic constraint and be as close as possible to satisfying the performance constraint,

$$T_i = \tilde{T}_i \qquad (20)$$

5.2 Optimizing The Cost Function Within Constraints

The cost function is evaluated over a three dimensional space. However if the series and parallel control distribution problems are separated, as described earlier, then each sub-problem will have reduced dimensionality. The series control distribution routine has one degree of freedom in the choice of T_o, and the parallel control routine has two degrees of freedom in distributing the load among the three motors. The parallel control distribution in terms of T_1, T_2, and T_o is:

$$\inf_{T_1,T_2}\ J_s\,(T_1,T_2) =$$

$$\inf_{T_1,T_2} \sum_{i=1}^{2} p\,(d_i\,(t+\tau) > \psi_i\,(t+\tau)\,|T_i) \quad (21)$$
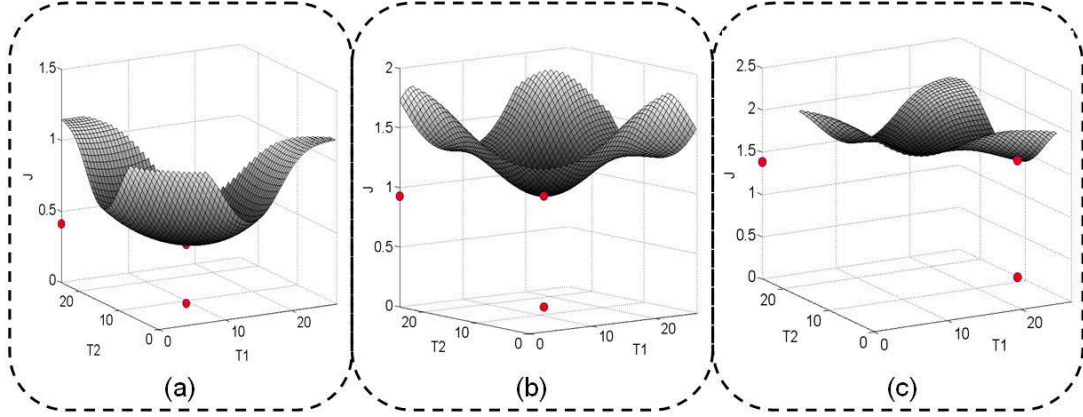
Figure 11: Plots of the parallel distribution cost function for $T_o = 0.4\tilde{T}$ (a), $T_o = 0.6\tilde{T}$ (b), and $T_o = 0.7\tilde{T}$ (c).

Eq. (21) is derived from the cost function defined in Eq. (15) with T_3 given implicitly in terms of T_1, T_2, and T_o:

$$T_3 = \frac{T_o}{\rho} - T_1 - T_2 \qquad (22)$$

Figure 11 shows plots of the parallel distribution cost function for low, moderate, and high load levels. Initial estimates for the insulation insulation healths were assigned to be normally distributed with $\sigma_i^2 = 1$, $\mu_1 = .05$, $\mu_2 = .35$, and $\mu_3 = .55$, where μ_i is the mean of the initial estimate for the health of motor i, and σ_i^2 is the corresponding variance. The surfaces shown in Figure 11 were created using these initial health estimates as well as $\tau = 1500$, and $\psi_i = 0.7$. As shown in the figure, the optimal prognostic cost is monotonically increasing with system load, and the healthier motors are assigned a greater proportion of the load.

Using the optimal the parallel distribution cost, the series control distribution routine will set the deviation from nominal performance, $|T_c - T_o|$, to minimize the sum of the performance and prognostic penalties. The performance penalty is monotonically increasing with performance degradation, and the the prognostic penalty, which is found via the parallel distribution routine is monotonically decreasing with performance degradation.

6. SIMULATION RESULTS

Simulation results are given using the initial winding degradations described in the previous section. A very demanding load speed profile is used, Figure 12, in order to observe significant winding degradation.

Simulation results are shown in Figure 13 for the receding horizon optimal control problem defined in Eq. (15) using the following parameters: $\tau = 50$ sec, $\lambda = 500\tau$, and $\psi_i(t + \tau) = (\phi_i(t + \tau) + d_i(t))/2$. Also the maximum fault growth curve, ϕ_i, is defined as a linear function from $\phi_i(t + \tau) = d(t)$ to $\phi_i(1500) = 0.9$.

The results of this simulation provide some insight into the nature of the receding horizon optimization approach. Qualitative remarks regarding the simulation results are given below.
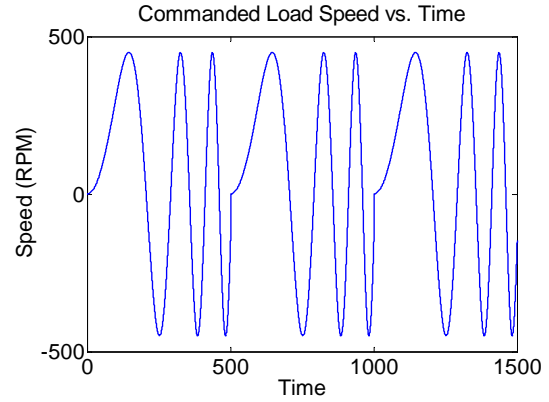

Figure 12: Load speed profile for EMA

Observation 1:   Using a relatively short prognostic horizon, $\tau = 50$ sec, causes the prognostic bound on motor torque, plotted in Figure 13 (a), to vary widely over the run. It tends to be looser when the winding temperature is low and tighter when the winding temperature is high because the winding's thermal capacitance protects the system from sharp increases in temperature.

Observation 2:   The performance constraint is violated during some of the more aggressive regions in the load speed profile, and the system is operated at 100% performance during the less aggressive parts of the cycle. This problem can be corrected by manipulating the maximum allowable fault growth curve; $\phi_i(t)$ is made steeper during the more aggressive parts of the cycle, and less steep during the less aggressive parts . Figure 14 shows results obtained using this type of piecewise linear design for $\phi_i(t)$. As shown in the figure, this extra degree of freedom enables a control to be found which does not violate the performance constraint. Future work is needed to create quantitative metrics for selecting this parameter and others based on assumptions about the fault growth model and mission profile.
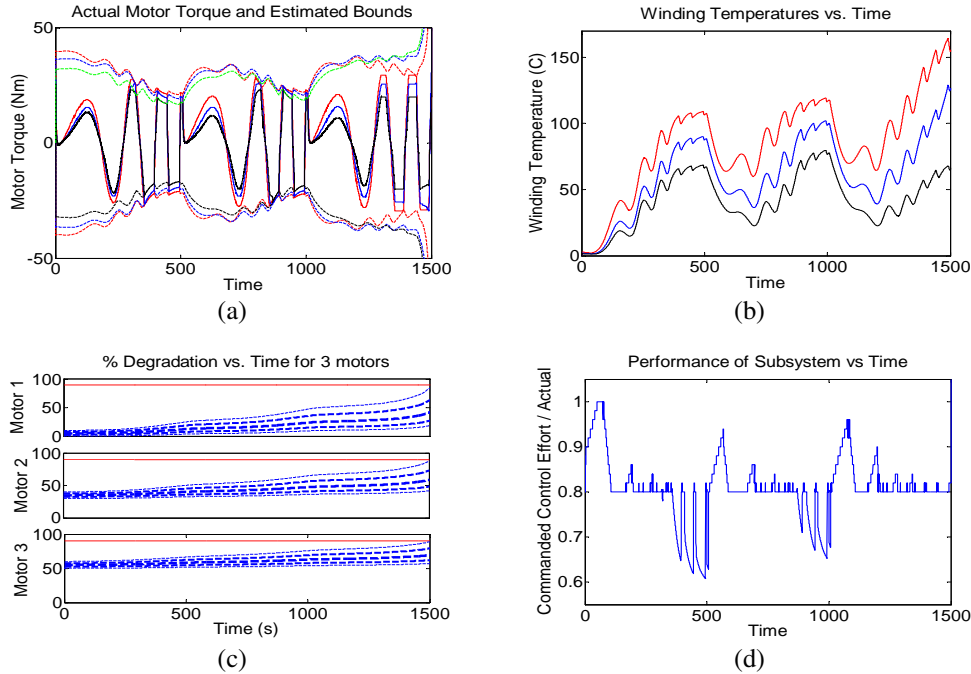
Figure 13: Simulation results using $\tau = 50$ sec, $\lambda = 500\tau$, $\phi_i(t+\tau) = $ linear, $\psi_i(t+\tau) = (\phi_i(t+\tau) + d_i(t))/2$. Plots show: motor torques (a), winding temperatures (b), insulation degradation pdfs (c) (lines represent mean and $\pm$ 2 standard deviations), and EMA performance (d).
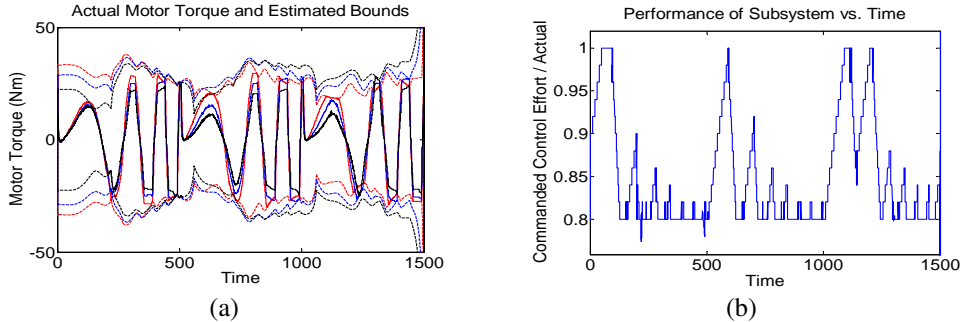

Figure 14: Plots of EMA motor torques (a) and performance (b) using piecewise linear constraint

7. CONCLUSION

A hierarchical architecture was discussed for setting up fault adaptive control of a generic overactuated system with embedded nominal controllers. A finite horizon bounded optimization problem was developed to redistribute load among a system's components, where specifications on maximum risk of failure and maximum degradation of nominal performance are used as constraints. The motivation for using a finite horizon optimization problem is that the cost function allows direct specification of the relative importance of maintaining nominal performance and minimizing risk. The development of this approach for a system with active redundant actuation was examined, and simulation results demonstrated the nature of the optimization problem. Research is underway to address computational issues and parameter selection for the finite horizon optimization problem. Future work will further explore the implementation of the presented architecture on EMA hardware, as well as exploring implementations on new systems, which may not not have active redundancy.

NOMENCLATURE

θ_c Commanded state vector
$\tilde{\theta}_c$ State vector commanded by high level control
θ_i State vector command seen by component i
θ_o Measured state vector
$\mathbf{u}_i$ Control signal for component i
y_i Component control effort output
$\mathbf{y}$ Net control effort output of subsystem
$\mathbf{r}$ Control effort commaned of the subsystem
σ Performance degradation term
$\tilde{\mathbf{r}}$ Mid-level control effort command for subsystem
$\tilde{\mathbf{r}}_i$ Mid-level control effort command for component i

REFERENCES

Arulampalam, M. S., Maskell, S., Gordon, N., & Clapp, T. (2002, Feb). A Tutorial on Particle Filters for Online Nonlinear/Non-Gaussian Bayesian Tracking. *IEEE Transactions on Signal Processing*, *50*(2), 174-188.

Bole, B. M., Brown, D., & Vachtsevanos, G. (2010). Automated Contengency Management (ACM) for Overactuated Systems.

Brown, D., Edwards, D., Georgoulas, G., Zhang, B., & Vachtsevanos, G. (2008). Real-Time Fault Detection and Accommodation for COTS Resolver Position Sensors. In *1st International Conference on Prognostics and Health Management (PHM)*.

Brown, D., Georgoulas, G., Bae, H., Chen, R., Y. Ho, G. T., Schroeder, J. B., et al. (2009). Particle filter based anomaly detection for aircraft actuator systems. In *IEEE Aerospace Conference.*

Brown, D., Georgoulas, G., Bole, B., Pei, H.-L., Orchard, M., Tang, L., et al. (2009, october). "Prognostics Enhanced Reconfigurable Control of Electro-Mechanical Actuators". In *2nd International Conference on Prognostics and Health Management (PHM).*

Drozeski, G. R. (2005). *A Fault-Tolerant Control Architecture for Unmanned Aerial Vehicles*. Unpublished doctoral dissertation, Georgia Institute of Technology.

Harkegard, O., & Glad, S. T. (2005, January). Resolving Actuator Redundancy - Optimal Control vs. Control Allocation. *Automatica*, *41*(1), 137-144.

Li, Y., Kurfess, T., & LIANG, S. (2000, September). Stochastic Prognostics for Rolling Element Bearings. *Mechanical Systems and Signal Processing*, *14*(5), 747-762.

Monaco, J. F., Ward, D. G., & Bateman, A. J. (2004, September). A Retrofit Architecture for Model-Based Adaptive Flight Control. In *AIAA 1st Intelligent Systems Technical Conference.*

Montsinger, V. M. (1930). Loading transformers by temperature. *Transactions of the American Institute of Electrical Engineers*, *32*.

.M.Zhang, Y., & J.Jiang. (2002). Active fault-tolerant control system against partial actuatorfailures. *IEE proceedings on control theory and applications*, *149*(149), 95.

Nestler, H., & Sattler, P. K. (1993, January). On-line estimation of temperatures in electrical machines by an observer. *Electric Power Components and Systems,*, *21*(1), 39-50.

Oppenheimer, M. W., Doman, D. B., & Bolender, M. A. (2006). Control allocation for over-actuated systems. In *14th Mediterranean Conference on Control and Automation.*

Orchard, M. (2007). *A particle filtering-based framework for on-line fault diagnosis and failure prognosis*. Unpublished doctoral dissertation, Georgia Institute of Technology.

Zhang, B., Georgoulas, G., Orchard, M., Saxena, A., Brown, D., Vachtsevanos, G., et al. (2008). Rolling Element Bearing Feature Extraction and Anomaly Detection Based on Vibration Monitoring. In *16th Mediterranean Conference on Control and Automation.*

Zhank, Y. M., & Jiang, J. (2002, January). Active fault-tolerant control system against partial actuator failures. *IEE Proc.-Control Theory Appl.*, *149*(1).

Brian M. Bole graduated from the FSU-FAMU School of Engineering in 2008 with a B.S. in ECE and a B.S. in Applied Math. He is pursuing a Ph.D. degree in electrical engineering at the Georgia Institute of Technology specializing in control systems. His research interests include multi-agent control, robust control, and adaptive control utilizing fault prognosis and diagnosis.

Douglas W. Brown received the B.S. degree in electrical engineering from the Rochester Institute of Technology in 2006 and the M.S degree in electrical engineering from the Georgia Institute of Technology in 2008. He is a recipient of the National Defense Science and Engineering Graduate (NDSEG) Fellowship and is currently pursuing the Ph.D. degree in electrical engineering at the Georgia Institute of Technology specializing in control systems. His research interests include incorporation of Prognostics Health Management (PHM) for fault-tolerant control. Prior to joining Georgia Tech, Douglas was employed as a project engineer at Impact Technologies where he worked on incipient fault detection techniques, electronic component test strategies, and diagnostics/prognostic algorithms for power supplies and RF component applications.

Hai-Long Pei is a Professor and Deputy Dean of the College of Automation Science and Engineering at South China University of Technology. He received the B.S. degree and the M. Sc. degree both in electronic engineering from the Northwestern Polytechnical University in China in 1986 and 1989 separately, and the Ph.D. degree in Automation from South China University of Technology in 1992. His research interest includes autonomous systems, intelligent control, and prognosis enhanced reconfiguration control.

Kai Goebel received the degree of Diplom-Ingenieur from the Technische Universität München, Germany in 1990. He received the M.S. and Ph.D. from the University of California at Berkeley in 1993 and 1996, respectively. Dr. Goebel is a senior scientist at NASA Ames Research Center where he leads the Diagnostics & Prognostics groups in the Intelligent Systems division. In addition, he directs the Prognostics Center of Excellence and he is the Associate Principal Investigator for Prognostics of NASA's Integrated Vehicle Health

Management Program. He worked at General Electric's Corporate Research Center in Niskayuna, NY from 1997 to 2006 as a senior research scientist. He has carried out applied research in the areas of artificial intelligence, soft computing, and information fusion. His research interest lies in advancing these techniques for real time monitoring, diagnostics, and prognostics. He holds ten patents and has published more than 100 papers in the area of systems health management.

Liang Tang Liang Tang is a Sr. Lead Engineer at Impact Technologies LLC, Rochester, NY. His research interests include diagnostics, prognostics and health management systems (PHM), fault tolerant control, intelligent control, and signal processing. He obtained a Ph.D. degree in Control Theory and Engineering from Shanghai Jiao Tong University, China in 1999. Before he joined Impact Technologies, he worked as a post doctoral research fellow at Intelligent Control Systems Laboratory, Georgia Institute of Technology. At Impact Technologies he is responsible for multiple DoD and NASA funded research and development projects on structural integrity prognosis, prognostics and uncertainty management, automated fault accommodation for aircraft systems, and UAV controls. Dr. Tang has published more than 30 papers in his areas of expertise.

George J. Vachtsevanos is a Professor Emeritus of Electrical and Computer Engineering at the Georgia Institute of Technology. He was awarded a B.E.E. degree from the City College of New York in 1962, a M.E.E. degree from New York University in 1963 and the Ph.D. degree in Electrical Engineering from the City University of New York in 1970. He directs the Intelligent Control Systems laboratory at Georgia Tech where faculty and students are conducting research in intelligent control, neurotechnology and cardiotechnology, fault diagnosis and prognosis of large-scale dynamical systems and control technologies for Unmanned Aerial Vehicles. His work is funded by government agencies and industry. He has published over 240 technical papers and is a senior member of IEEE. Dr. Vachtsevanos was awarded the IEEE Control Systems Magazine Outstanding Paper Award for the years 2002-2003 (with L. Wills and B. Heck). He was also awarded the 2002-2003 Georgia Tech School of Electrical and Computer Engineering Distinguished Professor Award and the 2003-2004 Georgia Institute of Technology Outstanding Interdisciplinary Activities Award.